S-adenosylmethionine synthases specify distinct H3K4me3 populations and gene expression patterns during heat stress

Adwait A. Godbole[1], Sneha Gopalan[2], Thien-Kim Nguyen[1], Thomas G. Fazzio[2], Amy K. Walker[1]

1. Program in Molecular Medicine, UMASS Chan Medical School, Worcester, MA 01605
2. Department of Molecular, Cell, and Cancer Biology, UMASS Chan Medical School, Worcester, MA 01605

Abstract

Methylation is a widely occurring modification that requires the methyl donor S-adenosylmethionine (SAM) and acts in the regulation of gene expression and other processes. SAM is synthesized from methionine, which is imported or generated through the 1-carbon cycle (1CC). Alterations in 1CC function have clear effects on lifespan and stress-responsive phenotypes, but specific mechanistic links have been difficult to identify because methylation is a widely distributed modification. Here we find that two SAM synthases in *Caenorhabditis elegans*, SAMS-1 and SAMS-4, contribute differently to modification of H3K4me3, gene expression and survival in the heat stress response. Both synthases are expressed in intestinal and hypodermal cells, which are major stress responsive tissues. We find that SAM is provisioned to distinct targets, even within the same methylation mark, depending on the enzymatic source. This suggests that determining how methyl donors are provided will broaden insight into 1CC functions in aging and stress.

Introduction

The 1-Carbon cycle (1CC) is a group of interconnected pathways that link essential nutrients such as methionine, folate and vitamin B12 to the production of nucleotides, glutathione, and S-adenosylmethionine (SAM), the major methyl donor (Ducker and Rabinowitz, 2016). SAM is important for the production of polyamines and phosphatidylcholine (PC), a methylated phospholipid, and is also essential for the methylation of RNA, DNA and proteins such as histones (Mato et al., 2008). Thus, 1CC connects nutrients with the production of a key cellular regulator of epigenetic function, SAM.

Alterations in 1CC function can cause a variety of defects (Ducker and Rabinowitz, 2016), including intriguing connections between this cycle, stress responses and aging. Lifespan lengthens in yeast, *C. elegans*, *Drosophila* and rodent models when methionine is restricted, genes in the methionine-SAM (Met-SAM) cycle are mutated, or polyamines are supplemented (Parkhitko et al., 2019). While multiple aspects of 1CC function could affect aging, the Met-SAM cycle has particularly strong links. For example, a *C. elegans* SAM synthase, *sams-1*, was identified in a screen for long-lived animals (Hansen, 2005) and multiple SAM-utilizing histone methyltransferases are also implicated as aging regulators (Greer et al., 2010; Han and Brunet, 2012; Han et al., 2017). Of thermoactive molecules, SAM is second only to ATP in cellular abundance (Ye and Tu, 2018), which raises the question of how such an abundant metabolite can exert specific phenotypic effects. Strikingly, studies in multiple organisms from a variety of labs have shown that reduction in SAM levels preferentially affects H3K4me3 levels

(Ding et al., 2015; Kraus et al., 2014; Mentch et al., 2015; Shyh-Chang et al., 2013). However, changes in SAM production may affect other histone modifications as well. For example, the Gasser lab showed that *sams-1* and *sams-3* have distinct roles in heterochromatin formation, which involves H3K9me3 (Towbin et al., 2012) A yeast SAM synthase has also been shown to act as part of the SESAME histone modification complex (Li et al., 2015) or to cooperate with the SIN3 repressor (Liu and Pile, 2017). In addition, most eukaryotes have more than one SAM synthase, which could allow partitioning of enzyme output by developmental stage, tissue type or cellular process and underlie specific phenotypic effects. Indeed, in budding yeast, SAM1 and SAM2 are co-expressed but regulated by different metabolic events, have distinct posttranslational modifications, and act differently in phenotypes such as genome stability (Hoffert et al., 2019). The two SAM synthases present in mammals are expressed in distinct tissues: MAT2A is present throughout development and in most adult tissues, whereas MAT1A is specific to adult liver (Maldonado et al., 2018). MAT2A may be present in distinct regulatory conformations with its partner MAT2B (Maldonado et al., 2018). However, the physiological impacts of these interactions are not clear. Studies exploring specificity of metazoan SAM synthase function have been difficult, as MAT1A expression decreases *ex vivo* and MAT2A is essential for cell viability (Mato et al., 2002). Finally, the high methionine content of traditional cell culture media has limited functional studies (Sullivan et al., 2021).

We have explored SAM synthase function in *C. elegans*, where the gene family has undergone an expansion. In *C. elegans*, genetic and molecular assays allow separation

of SAM synthase expression and function *in vivo*. Furthermore, no single SAM synthase is required for survival in normal laboratory conditions or diets. *sams-1* and the highly similar *sams-3*/*sams-4* are expressed in adult animals, whereas *sams-5* is present at low levels in adults and *sams-2* is a pseudogene (Harris et al., 2019). We previously found that *sams-1* had multiple distinct functions, contributing to PC pools and stimulating lipid synthesis through a feedback loop involving *sbp-1*/SREBP-1 (Walker et al., 2011) as well as regulating global H3K4me3 levels in intestinal nuclei (Ding et al., 2015). Our studies also showed that loss of *sams-1* produced different phenotypes in bacterial or heat stress. While *sams-1* was necessary for pathogen challenge, promoter H3K4me3 and expression of immune genes, animals surprisingly survived better during heat shock when they lacked *sams-1* (Ding et al., 2015). Because heat shocked animals require the H3K4me3 methyltransferase *set-16/MLL* for survival, we hypothesized that SAM from a different source may be important for histone methylation and survival in the heat shock response. Here, we find that SAM source impacts the functional outputs of methylation. While the SAM and the 1CC are well associated with regulation of lifespan and stress responses, direct molecular connections have been difficult to discover. Mechanisms controlling provisioning of SAM, therefore, could provide a critical level of regulation in these processes. We show that *sams-1* and *sams-4* differentially affect different populations of histone methylation and thus gene expression in the heat shock response, and that their loss results in opposing phenotypes. Our study demonstrates that SAM synthases have a critical impact on methylation targets and phenotypes associated with 1CC dysfunction. Thus,

defining the specificity of SAM synthases may provide a method to identify from broad effects methylation events that are specific phenotypic drivers.

Results

sams-1 and *sams-4* have overlapping and distinct expression patterns and gene regulatory effects

Animals respond to stress by activating specialized protective gene expression programs (Nadal et al., 2011). While these programs depend on specific signaling and transcriptional activators, they may also be impacted by histone methylation and the production of SAM. For example, we found that *C. elegans* lacking *sams-1* die rapidly on pathogenic bacteria, have low global H3K4me3 and fail to upregulate immune response genes (Ding et al., 2015). In contrast, heat shocked animals survive better without *sams-1* (Ding et al., 2018), with normal increases in heat shock genes accompanied by other broad changes in the transcriptome, including downregulation of many metabolic genes. We hypothesized that other SAM synthases could play an important role in mediating survival during heat shock (**Fig1A**), and focused on *sams-4*, which is also expressed at high levels in adult animals. Mass spectrometry assessment of SAM levels show a marked reduction after *sams-4* RNAi (**FigS1A**), demonstrating that like *sams-1* (Walker, 2011), it is a major contributor to SAM pools. RNA sequencing (RNAseq) shows that global gene expression patterns after *sams-1* or *sams-4(RNAi)* are distinct from each other (**FigS1B; Table S1: Tab B**). To determine if the enrichment of altered biological processes was also distinct, we used WormCat (Holdorf et al., 2019), which provides enrichment scores for three category levels (Cat1, Cat2, Cat3) for broad to more specific comparisons. WormCat finds that gene function

categories at the Cat1 and Cat 2 level, such as METABOLISM: Lipid or STRESS RESPONSE: Pathogen, are enriched at lower levels and contain different genes in *sams-4(RNAi)* animals (**Fig S1C-F, Table S1: Tabs D-F**). Notably, *fat-7* and other lipid synthesis genes that respond to low PC in *sams-1* animals are not upregulated after *sams-4(RNAi)* (**TableS1:Tab:B**). Finally, this strengthens the idea that these SAM synthases could have distinct functions.

In order to determine if *sams-1* and *sams-4* were expressed in similar tissues, we obtained strains where the C-termini of each protein was tagged with RFP or GFP, via CRISPR (**Fig1B**), and then used outcrossed animals to construct a *sams-1*::RFP; *sams-4*::GFP strain (**Fig1C**). SAMS-1::RFP fluorescence was evident in much of the adult animal, including intestine, hypodermis and cells in the head (**Fig1B, C**), in line with mRNA expression patterns derived from tissue-specific RNA seq (Kaletsky et al., 2018). However, SAMS-1::RFP was not present in the germline, which did express SAMS-4::GFP (**Fig1B, C**). SAMS-4::GFP was also present in intestinal and hypodermal cells (**Fig1B, C**), demonstrating that these tissues, which are major contributors to the stress response (McGhee, 2007) contain both of these SAM synthases.

Opposing roles and requirements for *sams-1* and *sams-4* in the heat shock response

Animals respond to stress by activating specialized protective gene expression programs (Nadal et al., 2011). While these programs depend on specific signaling and transcriptional activators, they may also be impacted by histone methylation and the

production of SAM. We previously found that *sams-1(RNAi)* animals exhibit more robust survival after heat shock, although these animals succumbed rapidly to bacterial infection (Ding et al., 2018). However, the H3K4me3 methyltransferase *set-16*/MLL was essential for survival after heat shock (Ding et al., 2018), suggesting that methylation was required. In order to determine if *sams-4* contributed to survival in heat shock, we compared the phenotypes of *C. elegans* with deletions in *sams-1* and *sams-4* to avoid co-targeting effects. *sams-4(ok3315)* animals have a deletion that removes around a third of the open reading frame. Unlike *sams-1(lof)* animals, *sams-4(ok3315)* mutants died rapidly after heat shock (**Fig1D, E; FigS1G; Table S2:Tabs B, C**). RNAi constructs targeting *sams-4* also can affect *sams-3* (Towbin et al., 2012)(see also **Table S1: Tabs A, B**), which is expressed in the opposite direction from the same promoter. However, these findings suggest *sams-4* depletion is the primary basis of the heat shock phenotypes and validate use of this RNAi strain to examine *sams-4* function. Finally, *sams-4(RNAi)* phenotypes in the heat stress response were not linked to a general failure to thrive, as *sams-4(RNAi)* animals under basal conditions had modestly enhanced lifespan (**FigS1G; Tab A**).

Next, we used immunostaining to compare global levels of H3K4me3 in *sams-1* and *sams-4* RNAi nuclei during heat shock. Although H3K4me3 deposition is independent *of sams-4* in embryonic nuclei (Towbin et al., 2012), it is broadly decreased in *sams-4(RNAi)* intestinal nuclei in basal conditions (15°C), as in *sams-1(RNAi)* (Ding et al., 2015) or *sams-1(ok3035) (sams-1(lof))* animals (**Fig1F-I)**. Surprisingly, we detected robust levels of H3K4me3 in *sams-1(lof)* nuclei after heat shock (2 hours at 37°C)

(**Fig1F, G**), suggesting that *sams-1*-independent mechanisms act on H3K4me3 during heat shock. These increases in H3K4me3 did not appear in heat shocked *sams-4(RNAi)* intestinal nuclei (**Fig1 H, I**), raising the possibility that *sams-4* contributed to the effects in *sams-1(lof)* animals. Next, we wanted to test effects of reducing both *sams-1* and *sams-4* levels on H3K4me3 during heat shock. Loss of multiple SAM synthases reduces viability in *C. elegans* (Towbin et al., 2012). In order to circumvent this, we used dietary choline to rescue PC synthesis and growth of *sams-1(RNAi)* or *(lof)* animals (Ding et al., 2015; Walker et al., 2011). *sams-1(lof); sams-4(RNAi)* animals were raised on choline until the L4 stage, then moved to normal media for 16 hours before heat shock. Immunostaining of *sams-1(lof); sams-4(RNAi)* intestines showed that *sams-4* is required for the H3K4me3 in heat shocked *sams-1(lof)* nuclei (**Fig1J, K**). These results suggest that H3K4me3 may be remodeled during heat shock with SAM from distinct synthases and that *sams-4*-dependent methylation is critical for survival.

Histone methyltransferase and histone demethylation machinery have modest, separable effects on *sams* mutant heat shock phenotypes

SAM is necessary for histone methylation; however, histone methylation dynamics are also influenced by methyltransferase (KMT) or demethylase (KDMT) activity (Bannister and Kouzarides, 2011). H3K4me3 is catalyzed by the COMPASS complex (Shilatifard, 2012). In mammals, seven methyltransferases in the SET1, MLL or THX groups can methylate H3K4. *C. elegans* contain single orthologs from each of these groups: *set-2/*SET1, *set-16*/MLL and *ash-2*/TXH, respectively, with roles in embryonic development (Li and Kelly, 2011; Wenzel et al., 2011; Xiao et al., 2011), lipid accumulation and

transgenerational inheritance (Greer et al., 2010; Han et al., 2017). *C. elegans* have multiple H3K4 KDMTs that function in development (Lussi et al., 2016) and aging (Alvares et al., 2014; Greer et al., 2010). Of these enzymes, we focused on KMTs *set-2* and *set-16* which are critical for wild type levels of H3K4me3 in intestinal nuclei (Ding et al., 2018) although *set-2* RNAi produces a more extensive loss of H3K4me3 and *set-16* a broader requirement for survival during stress. Because specificity for H3K4 mono, di or trimethylation has not been verified on a genome-wide scale for KDMTs, we examined multiple members of the H3K4 KDM family.

In order to determine if KMTs or KDMT dynamics played a role in the change of H3K4me3 during heat shock, we used RNAi to deplete them in *sams-1(lof)* or *sams-4(ok3315)* animals, measured survival after heat shock and intestinal H3K4me3 levels. RNAi of *set-2/SET1* or *set-16/MLL* increased survival in *sams-1(lof)* animals after heat shock (**FigS2A,D; Table S2:Tabs:C, E**) and did not limit heat shock-induced H3K4me3 in *sams-1(RNAi)* nuclei (**FigS2B-F**). RNAi of two KDMTs, *rbr-2* (**FigS2G**) and *spr-5* (**FigS2H**) had opposite effects from the KMTs, moderately reducing survival (**TableS2:Tab F**), whereas *amx-1* and *lsd-1* had no effect (**TableS2:Tabs I, J**). RNAi of *set-2* (**FigS2I**)or *set-16* (**FigS2J**) had slight, but statistically significant effects, increasing survival of *sams-4(ok3315)* animals (**TableS2:Tabs G, H**). However, survival was still significantly below controls in *sams-4(ok3315)* with or without the KMT RNAi. Taken together, this suggests that the H3K4me3 appearing after heat shock may contribute to with survival and that this methylation does not depend on a single methyltransferase or demethylase.

Distinct patterns of H3K4me3 and gene expression in *sams-1(RNAi)* versus *sams-4(RNAi)* animals during heat shock

H3K4me3 is a prevalent modification enriched near the transcription start sites (TSSs) of actively expressed genes (Eissenberg and Shilatifard, 2010). Differing global patterns of H3K4me3 in *sams-1(RNAi)* and *sams-4(RNAi)* nuclei suggest this histone modification at specific sites could also be distinct. In order to identify loci which might link H3K4me3 to these phenotypes, we used CUT&Tag, (Cleavage Under Targets and Tagmentation, C&T) (Kaya-Okur et al., 2019a), to determine genome-wide H3K4me3 levels. C&T is uniquely suited to the small sample sizes available from these stressed populations. In this approach, a proteinA-Tn5 transposase fusion protein binds to the target antibody in native chromatin and DNA libraries corresponding to antibody binding sites are generated after transposase activation. Sequencing and H3K4me3 libraries showed robust mapping to promoter-TSS regions (**Fig2A; TableS3:Tabs A-F**), validating this approach. TSS distributions were similar in basal and heat shocked animals, although heat shocked *sams-4(RNAi)* animals had fewer overall peaks (**Fig2B**). Next, we examined H3K4me3 TSS localization in Control (empty vector) RNAi animals and found moderate reductions occurred with heat shock. In particular around 20-30% were specific to animals at basal (15°C) vs. at heat shock (37°C) temperature (**Fig2C)**, suggesting that H3K4me3 could be remodeled upon heat shock in *C. elegans*.

In order to compare how *sams-1* or *sams-4* RNAi might affect H3K4me3 peak distribution, we performed TSS aggregations, and included also analysis of Control

RNAi samples. Overall, TSS localization dropped sharply in both *sams-1* and *sams-4* samples at 15°C, however this difference was less marked in heat shocked animals, due to lower TSS localization in Control animals (**Fig2D, E**). While overall TSS aggregation for H3K4me3 was similar for *sams-1* and *sams-4* RNAi animals, similar patterns could obscure distinct sets of H3K4me3 marked genes in each condition. Indeed, around 1000 peaks appear specific to Control or *sams-1* and around 500 in *sams-4* chromatin at 15°C with moderate increases in these numbers after heat shock. As H3K4me3 is a widely occurring modification, we hypothesized that we might better understand potential SAM synthase-specific requirements if we focused on peaks that change in the Control RNAi heat shock response and asked how they are affected by loss of *sams-1* or *sams-4*. We used two different methods for comparing potential SAM synthase requirements for H3K4me3 in the heat shock response. First, we used differential peak calling (ChIPPeakAnno (Zhu et al., 2010)) followed by WormCat category enrichment to determine the classes of genes which might be affected (**FigS3A-F; TableS3; Tabs G-I**). Peaks present in both basal and heat shocked conditions enriched for genes in the METABOLISM category (including Lipid: phospholipid, sphingolipid, sterol and lipid binding, along with mitochondrial genes) as well as in core function categories such as those involved in trafficking, DNA or mRNA functions (**Fig2F, FigS3D-E; Table S3: Tabs G-I)**. There was no significant category enrichment specific to 15°C animals, but after heat shock, Control RNAi animals gain enrichment in peaks at the Category 1 level in PROTEOSOME PROTEOLYSIS (**Fig2F**). This enrichment was driven by increases in H3K4me3 at E3: Fbox genes (**FigS3D-E; Table S3:Tab A,B**), which could be important for eliminating mis-folded proteins during

heat shock. Comparison of peaks differentially present in *sams-1* and *sams-4* RNAi animals showed that only *sams-1(RNAi)* exhibited a similar enrichment to Control RNAi in the PROTEOLYSIS PROTEOSOME category (**Fig2G, FigS3E, F**), which could help explain the reduced survival of *sams-4(RNAi)* animals relative to *sams-1(RNAi)* animals. *sams-1* RNAi animals also gained enriched peaks in a wide range of gene categories within METABOLISM, whereas *sams-4(RNAi)* enriched peaks in these categories were more limited (**FigS3C-F**). Thus, loss of *sams-1* or *sams-4* differentially affects H3K4me3 peaks within functional gene classes that also change in the heat shock response.

Next, we hypothesized that H3K4me3 at peaks in Control RNAi animals might exist as multiple differently regulated populations, some which are linked to SAM synthase function and others that are regulated by different mechanisms. In order to test this, we divided peaks in Control animals at 15°C or 37°C into those that did not change after SAM synthase RNAi (*sams-1* or *sams-4* independent peaks) or those that were dependent on *sams-1* or *sams-4* and examined aggregations around TSS regions. There was little difference between TSS plots of *sams-1* or *sams-4*-independent genes at either temperature (**Fig2H, I**). However, in basal conditions, Control peaks that depended on *sams-1* had more marked TSS localization (**Fig2J**), demonstrating that *sams-1* and *sams-4* dependent peaks have distinct TSS architectures. TSS localization was low in all 37°C samples, following the general trend of decrease after heat shock (**Fig2K**). We next separated Control peaks into those that were generally SAM synthase-dependent and those that were specific to loss of *sams-1* or *sams-4*.

Aggregation of these peaks shows that peaks in Control 15°C samples that were lost only in *sams-4* RNAi also had the lowest levels of H3K4me3 in TSS regions, whereas promoters that lost this modification only after *sams-1* RNAi had higher levels of H3K4me3 (**FigS3G**). Control 37°C samples exhibited a similar pattern, with a lower H3K4me3 level overall consistent with what we have observed in heat shock samples (**FigS3H**). Thus, genome-wide H3K4me3 contain multiple populations with distinct TSS patterns. Peaks that are present even when *sams-1* or *sams-4* are depleted have the highest levels, whereas *sams-1*-dependent peaks have moderate H3K4me3, and peaks that are lost after *sams-4* RNAi have the lowest levels. Taken together, this shows that individual SAM synthases are linked to distinct sets of H3K4me3 within the genome.

RNAi of *sams-1* or *sams-4* has similar effects on TSS peaks at tissue-specific genes

Our C&T and RNA seq assays were performed on whole animals. While *sams-1* and *sams-4* are co-expressed in the intestine and hypodermis, which are major stress-responsive tissues, the germline nuclei contain only *sams-4*. This aligns with our previous observations that *sams-1(RNAi)* animals had normal patterns of H3K4me3 in germline nuclei (Ding, et al. 2015), whereas RNAi of *sams-4* abrogates H3K4me3 staining in germline nuclei (**FigS4A**). However, embryo production and development appears broadly normal in *sams-4* RNAi embryos (not shown). In order to determine how H3K4me3 might align with tissue-specific expression patterns, we aggregated peaks from tissue-specific RNA seq data published by Serizay, et al (Serizay et al., 2020). Serizay et al. separated nuclei based on tissue specific GFP expression and

defined gene sets that were expressed that were ubiquitously, as well as those that were present only in a single tissue. They also performed ATAC seq (Assay for Transposase-Accessible Chromatin using sequencing). Serizay, et al. defined transcripts by expression pattern and defined sets that were specific to (*tissue*_only), or represented in across multiple tissues (*tissue*_all). ubiquitious_all and Germline_only genes had the most defined patterns of open chromatin around TSSs (Serizay et al., 2020) We compared our C&T data with Ubiquitious_all, Germline_only and Intestine_only genes and found that we identified peaks for around half of these genes in Control RNAi animals at 15°C or 37°C (**FigS4B-D)**. We found the ubiquitous_all and germline_only genes also had strong H3K4me3 peaks that were reduced equally by *sams-1* or *sams-4* RNAi in both temperature conditions (**FigS4D, G; E, H**). Intestine_only genes showed lower TSS enrichment but were similarly reduced after *sams-1* or *sams-4* RNAi (**FigS4H, I**). This data suggests that differences in germline expression for *sams-1* and *sams-4* are not sufficient to explain differential effects on H3K4me3 peak populations.

Poor expression of heat shock gene suite in *sams-4(RNAi)* animals

H3K4me3 is found at the promoters of many actively transcribed genes, but it is not necessarily required for gene expression (Bannister and Kouzarides, 2011). However, studying chromatin modification in stress responses may reveal additional regulatory effects (Weiner et al., 2012). We previously found using ChIP-PCR in the context of the stress response in *C. elegans* that H3K4me3 increased at promoters of genes that responded to bacterial stress in a *sams-1*-dependent manner (Ding, et al. 2015).

However, during the stress response, H3K4me3 did not change at multiple non-stress responsive genes, suggesting that stress-responsive loci might be more sensitive to SAM levels (Ding, et al. 2015). In order to identify genes that changed in SAM-deficient animals, we performed RNA seq, then compared genes induced by heat shock in control and *sams-1(RNAi)* (Ding, et al. 2018) with genes induced in *sams-4(RNAi)* animals **(TableS4: A-C**). We previously noted that while *sams-1(RNAi)* animals could not mount the full transcriptional response to bacterial stress, most genes activated by heat increased similarly to controls (Ding, et al. 2018). *sams-4(RNAi)* animals, in contrast, activate less than 25% of the genes induced by heat in control animals (**Fig3A**). *sams-1(RNAi)* and *sams-4(RNAi)* animals also induce more that 600 genes in response to heat that are SAM-synthase-specific and which do not increase in control animals (**Fig3A**). WormCat pathway analysis shows that *sams-4(RNAi)* animals lack the robust enrichment in STRESS RESPONSE (Cat1) and STRESS RESPONSE: Heat (Cat2) evidenced in both Control and *sams-1(RNAi)* samples (**Fig3B; TableS4: D-F**). In addition, enrichment of the CHAPERONE, PROTEOLYSIS PROTEOSOME categories occurring in *sams-1(RNAi)* animals does not occur after *sams-4(RNAi)*, reflecting lack of induction of these genes which could be important for proteostasis in the heat shock response (**Fig3C**). Thus, reduction in *sams-1* or *sams-4* results in distinct gene expression programs in both basal conditions (**FigS1B-F**) and during the heat stress response (**Fig3A-C**). This differentiation of gene expression programs clearly shows that *sams-1* and *sams-4* have distinct functional roles.

Gene expression changes occurring after *sams-1* or *sams-4* depletion could result from direct effects on H3K4me3 or other potential methylation targets, or from indirect effects. Evaluating the impact H3K4me3 on gene expression is also complex, as this modification is generally associated but not necessary for expression of actively transcribed genes (Bannister and Kouzarides, 2011). In our analysis of H3K4me3 peaks during the heat stress response, we found evidence of multiple peak populations that depend on or occur independently of *sams-1* or *sams-4* (**Fig2H-K, FigS3A-F**). We reasoned, therefore, that it was also critical to determine H3K4me3 levels at *sams-1-* or *sams-4*-dependent genes in the heat shock response.

First, we examined H3K4me3 peak levels at genes with increased in Control RNAi, *sams-1(RNAi)* or *sams-4(RNAi)* during heat shock. We found that genes dependent on *sams-1* or *sams-4* in the heat shock response were marked by lower overall H3K4me3 levels at the TSSs (**Fig3D**). However, this analysis included large numbers of upregulated genes in *sams-1* or *sams-4* outside of the wild type heat stress response. Therefore, we next focused on genes normally upregulated during heat shock and divided them according to SAM synthase dependence. Strikingly, isolating the *sams-1*-dependent genes revealed a strong peak 5 prime to the TSS, which was not evident in the larger subset of Control or *sams-4(RNAi)*-dependent upregulated genes (**Fig3E, F**). Among the genes with robust peaks in heat shocked *sams-1(RNAi)* animals were two F-box proteins, *fbxa-59* and T27F6.8, which were robustly expressed in *sams-1* but not *sams-4* animals (**Fig3C, G-I**). While survival in heat shock is likely to be multi-genic and may rely on pathway responses rather than single genes, our data shows genes

upregulated in the heat shock response may have different H3K4me3 levels depending on if the genes are require *sams-1* or *sams-4*. This provides additional evidence of distinct requirements for *sams-1* and *sams-4* for the induction of genes during heat stress. In addition, our results suggest that roles for H3K4me3 may become clearer when genome-wide methylation populations are separated into biologically responsive categories.

SAM synthase-specific effects on genes downregulated in the heat shock response

Transcriptional responses to heat shock largely focus on rapidly induced genes that provide protection from changes in proteostasis (Mahat et al., 2016; Morimoto, 2006). However, downregulated genes could also play important roles. For example, the WormCat category of TRANSMEMBRANE TRANSPORT (TM TRANS) is enriched in genes downregulated after heat shock in *C. elegans* (Ding, et al 2018; **Fig4A,B**). Previously we observed that heat shocked animals depended on *sams-1* for normal expression of nearly 2,000 genes, falling within WormCat Categories of METABOLISM, TRANSCRIPTION FACTOR (TF), SIGNALLING and STRESS RESPONSE (**Fig4A,B**). Interestingly, the metabolic genes dependent on *sams-1* include those in lipid metabolism, whereas the TF enrichment was centered around nuclear hormone receptors (NHRs) (**Fig4C,D**) (Ding, et al. 2018), which regulate many metabolic and stress responsive genes in *C. elegans* (Arda et al., 2010). However, neither the shared TM TRANSPORT nor the *sams-1* specific categories depend on *sams-4* (**Fig4A-E**).

Thus, as in genes upregulated during the heat shock response, genes downregulated in the heat shock response also have differential requirements for *sams-1* and *sams-4*.

Next, we examined H3K4me3 levels around TSSs of genes that lost expression during heat shock in Control, *sams-1* or *sams-4(RNAi)* animals. Genes decreasing in Control animals had a slight reduction of H3K4me3 peaks when comparing15°C and 37°C samples, consistent with global levels after heat shock (**Fig4D**). RNAi of *sams-1 or sams-4* also broadly reduced H3K4me3 TSS enrichment at downregulated genes (**Fig4E, F**). However, there were minimal differences before or after heat shock. Because H3K4me3 has been reported to act as a bookmarking modification, we hypothesized that some loci could be affected before heat shock, with expression changing afterward. Therefore, we more closely examined genes with *sams-1*-dependent H3K4me3 at 15°C that lost expression during heat shock (**Fig4I**). Those genes were highly enriched for METABOLISM: Lipid: beta oxidation and NHR transcription factors (**Fig4G, H**). We noted they included multiple members of a regulatory circuit that control expression of a beta-oxidation-like pathway (**Fig4H**) that degrades toxic fatty acids identified by the Walhout lab (Bulcha et al., 2019), including *nhr-68*, *nhr-114* and beta-oxidation genes *acdh-1, hach-1 ech-6, -8,* and *-9*. Indeed, *nhr-68*, the initiating TF in this regulatory circuit, shows lower levels of H3K4me3 at its promoter in basal conditions, compared to Control or *sams-4* RNAi animals (**Fig4J**). The H3K4me3 peak overlaps with another gene, *pms-2*, whose expression does not change after heat shock or upon SAM synthase RNAi (**TableS4:Tabs A-C**). While the H3K4me3 peak at *nhr-68* does increases after heat shock in *sams-1* animals, consistent

with immunostaining, this is not sufficient to drive expression, which may require additional inputs. Thus, differences in H3K4me3 patterns in *sams-1* and *sams-4* animals before heat shock may also influence gene expression patterns during the stress response (**FigS4J**). Taken together, these results demonstrate that *sams-1* and *sams-4* are required for distinct sets of genes in the heat stress response and contribute to different H3K4me3 patterns.

Discussion

The molecules that modify chromatin are produced by metabolic pathways (Cheng and Kurdistani, 2022). Use of ATP, AcetylCoA or SAM for phosphorylation, acetylation or methylation of histones is tightly regulated and many studies have focused on control of enzymes or enzyme-containing complexes. Acetylation and methylation may also be regulated by metabolite levels (Hsieh et al., 2022; Wellen et al., 2009). This allows the chromatin environment to sense and respond to changes in key metabolic pathways. However, effects of methylation on chromatin are multifaceted: DNA and H3K9me9 have strong repressive effects, whereas other modifications such as H3K4me3 H3K36me3 are associated with active transcription (Bannister and Kouzarides, 2011). These marks, especially H3K4me3, are most sensitive to SAM levels, most likely due to the kinetics of the H3K4me3 MTs (Mentch and Locasale, 2016). SAM is an abundant metabolite that contributes to multiple biosynthetic pathways in addition to acting as the major donor for histone, DNA and RNA methylation (Walsh et al., 2017). Reduction in SAM levels has major phenotypic consequences in animals, altering lipid levels in

murine liver and *C. elegans* (Lu et al., 2001; Walker et al., 2011), altering differentiation potential in iPS cells (Shyh-Chang et al., 2013) and changing stress resistance (Ding et al., 2018). In addition, 1CC has been identified as a causal regulator of aging (Annibal et al., 2021) and is important in cancer development (Gao et al., 2019; Sullivan et al., 2021). However, the abundance of SAM and its targets have made it difficult to connect changes in methylation to these physiological effects. In addition, studying effects of SAM is difficult in culture because SAM itself is labile (Sun and Locasale, 2021) and tissue culture media is replete with 1CC metabolites (Sullivan et al., 2021). Important insights have been made into the impact of SAM on the breadth of H3K4me3 peaks using methionine depletion (Dai et al., 2018; Mentch et al., 2015; Tang et al., 2017), however, this approach could affect other pathways. In this study, we have taken the approach of limiting SAM synthase expression in *C. elegans*, then using genetic and molecular approaches to link methylation-dependent pathways to changes in stress responses. We found that individual SAM synthases could have distinct effects even on a single methylation target such as H3K4me3. This observation not only shows that examining how SAM is produced within the cells allows differentiation of phenotypic effects, but also supports the striking notion of 'where' SAM comes from affects its functional output. While mammalian cells express either one of two SAM synthases, MAT2A, which is present in non-liver cells, may be present in multiple regulatory isoforms (Murray et al., 2019). Thus, the isoform-specific production and functional targets for SAM synthases we uncover could also be important in mammals. Hints of this exist in other cellular systems – 1CC enzymes, for example, have been associated

with chromatin modifying complex in yeast (Li et al., 2015) and mammalian cells (Greco et al., 2020).

H3K4me3 is clearly an important link between SAM levels, aging and stress phenotypes, as loss or reduction of H3K4 MT function phenocopy aspects of SAM depletion (Ding et al., 2015, 2018). However, this modification is also wide-spread and transcription may occur even when this mark is not present (Hödl and Basler, 2012). By studying acute changes in gene expression during heat stress response in *C. elegans*, we have found that H3K4me3 populations can also be separated based on SAM synthase requirements. SAM synthase-specific effects may also vary according to the biological context, as loss of *sams-1* improves the ability of *C. elegans* to survive heat stress, while limiting its ability to withstand bacterial pathogens (Ding et al., 2018). Notably, neither *sams-1* or *sams-4(RNAi)* altered H3K4me3 at *hsp* genes when measured directly after heat shock, although *hsp* genes, along with other chaperones or genes that could be linked to proteostasis, were expressed at lower levels. This suggests there may not be single “target genes” that directly link H3K4me3 to survival, but that the phenotypic links lie in systems or pathway-level effects.

In summary, our study demonstrates that distinct gene expression, methylation and phenotypic outcomes can be linked to individual SAM synthases expressed within the same cells. Thus, understanding how and where SAM is produced may clarify the molecular basis of how the 1CC connects to phenotypes in aging and stress.

Limitations:

The genetic tools used in our study provide a method to reduce SAM from a specific enzymatic source. However, the roles for SAM in the cell are broad and can affect methylation of multiple targets. In addition, survival benefits after heat shock occur across broad cellular functions including proteostasis and other methylation marks such as H3K9me3 (Das et al., 2021). Thus there may be multiple additional methylation-dependent mechanisms that influence survival of *sams-1* or *sams-4* animals during heat shock. In addition, we measured gene expression and H3K4me3 at two hours post heat shock, whereas the survival assay occurs over multiple days. Thus, there may be changes in gene expression or histone modifications occurring at later times that also affect survival.

Materials and methods

C. elegans culture, RNAi and stress applications.

C. elegans (N2) were cultured using standard laboratory conditions on *E. coli* OP50. Adults were bleached onto RNAi plates and allowed to develop to the L4 to young adult transition before stresses were applied. For heat stress applications, animals were raised at 15°C from hatching then at the L4/young adult transition replicate plates were placed at 15°C or 37°C for 2 hours. After each stress, animals were washed off the plates with S-basal, then pellets frozen at -80°C. RNA was prepared as in (Ding et al., 2015). For survival assays, animals remained on plates until all nematodes were dead. Exposure to heat occurred for 120 minutes, then animals were kept at 20°C for the remainder of the assay. Dead animals were identified by gentle prodding and removed each day. Kaplan-Meir curves were generated with GraphPad Prism v5.0.

Gene expression analysis, RNA sequencing and analysis

Young adult *C. elegans* were lysed in 0.5% SDS, 5% b-ME, 10 mM EDTA, 10 mM Tris-HCl pH 7.4, 0.5 mg/ml Proteinase K, then RNA was purified with Tri-Reagent (Sigma) (Walker et al., 2011). cDNA for quantitative RT-PCR was prepared with the Invitrogen Transcriptor kit. cDNA was standardized to *act-1*. Graphs represent representative experiments selected from at least three biological replicates. Two-tailed Student's t tests were used to compare significance between values with two technical replicates. Primer sequences are available upon request.

RNA for deep sequencing was purified by Qiagen RNAeasy. Duplicate samples were sent for library construction and sequencing at BGI (China). Raw sequencing reads were processed using an in-house RNA-Seq data processing software Dolphin at University of Massachusetts Medical School (Yukselen et al., 2020). The raw read pairs were first aligned to *C. elegans* reference genome with ws245 annotation. The RSEM method was used to quantify the expression levels of genes and Deseq was used to produce differentially expressed gene sets with more than a 2-fold difference in gene expression, with replicates being within 0.05 in a Students T test and a False Discovery Rate (FDR) under 0.01. Statistics were calculated with DeBrowser (Kucukural et al., 2019). Venn Diagrams were constructed by BioVenn (Hulsen et al., 2008).

Immunofluorescence

For H3K4me3 (RRID: AB_836882) staining, dissected intestines were incubated in 2% paraformaldehyde, freeze cracked, then treated with -20^{0}C ethanol before washing in PBS, 1% Tween-20, and 0.1% BSA. Images were taken on a Leica SPE II at identical gain settings within experimental sets. Quantitation was derived for pixel intensity over nuclear area for at least seven dissected intestines, with at least 3 nuclei per intestine. Three biological repeats were carried out for every experiment.

CUT&Tag

C. elegans (N2) were cultured using standard laboratory conditions on *E. coli* OP50. Adults were bleached onto RNAi plates and allowed to develop to the L4 to young adult transition before stresses were applied. For heat stress applications, animals were

raised at 15°C from hatching then at the L4/young adult transition replicate plates were placed at 15°C or 37°C for 2 hours. At the end of the heat stress, animals were washed off the plates with S-basal, then pellets frozen at -80°C. CUT&Tag protocol (Kaya-Okur et al., 2019b) with minor modifications was followed to generate sequencing libraries to determine the H3K4me3 landscape in basal and heat stress condition in worms fed on control, *sams-1* or *sams-4* RNAi (Kaya-Okur et al., 2019). Sequencing of the prepared libraries was carried out on Illumina NextSeq 500.

Data analysis

Paired end reads from each sample were aligned to the *C. elegans* genome (ce11 with ws245 annotations) using Bowtie2 (Langmead et al., 2009)with the parameters -N 1 and -X 2000. Duplicate reads were removed using Picard (http://broadinstitute.github.io/picard/) and the reads with low quality scores (MAPQ < 10) were removed. HOMER software suite was used to process the remaining mapped reads (Heinz et al., 2010). The “makeUCSCfile” command was used for generating genome browser tracks, the “findPeaks” command was used for calling H3K4me3 peaks and the “annotatePeaks” command was used for making aggregation plots. Differential peak calling was accomplished using ChipPeakAnno (Zhu et al., 2010). TSS plots were generated using HOMER (Heinz et al., 2010) and Venn Diagrams were constructed by BioVenn (Hulsen et al., 2008).

Acknowledgements

We would like to acknowledge the Walker lab for reading of the manuscript, Drs. Marian Walhout and Craig Peterson for helpful discussions and Life Science editors for manuscript assistance. Funding is from NIH: 1R01AG053355 to AKW and R01HD072122 to TGF.

Figure legends

Fig.1 *sams-1*-independent acquisition of H3K4me3 in heat shocked animals

(A) Methionine intake through diet enters the 1 carbon cycle and is used by SAM synthases for the synthesis of SAM which is used by methyltransferases to add methyl moieties to proteins, nucleic acids and lipids. **(B)** Representative confocal images of animals expressing SAMS-1::RFP or SAMS-4::GFP. **(C)** Representative confocal images of animals co-expressing SAMS-1::RFP and SAMS-4::GFP in hypodermis (h), sc (seam cell), sp (spermatheca) and intestine (i). (**D & E)** Kaplan-Meier survival plots of *sams-1(lof)* (b) or *ok3315* (c) following heat shock. Statistical significance is shown by Log-rank test. Each assay was repeated thrice, and the graph represents the average of 3 biologically independent repeats. (**F, H & J)** Representative immunofluorescence images of intestinal nuclei stained with H3K4me3-specific antibody. Immunofluorescence staining was carried out to quantify the level of H3K4me3 in intestinal nuclei with and without heat shock in animals fed control RNAi, *sams-4(RNAi)* or in *sams-1(lof)* animals. **(G, I and K)** Quantification of immunofluorescence imaging of intestinal nuclei stained with HK4me3 antibody with and without heat shock. Statistical significance was calculated using unpaired Student's t-test. ns= not significant, **** = $p<0.0001$, *** = $p<0.001$. Graph represents average of three biologically independent repeats per condition.

Fig.2 H3K4me3 modifying enzymes modulate SAM synthase phenotypes

(A) Bar graph showing the distribution of the enrichment of H3K4me3 over different genomic loci in animals fed control RNAi, *sams-1(RNAi)* or *sams-4(RNAi)* at 15°C and

37°C. **(B)** Aggregation plots showing TSS enrichment in the H3K4me3 peaks identified in animals fed control RNAi at 15°C and 37°C. **(C)** Venn diagram comparing the overlap in the H3K4me3 peaks identified in animals fed control RNAi at 15°C and 37°C. **(D)** Aggregation plots showing TSS enrichment in the H3K4me3 peaks identified in animals fed control RNAi or *sams-1(RNAi)* or *sams-4(RNAi)* at 15°C and Venn diagram comparing the overlap in the H3K4me3 peaks identified in animals fed control RNAi or *sams-1(RNAi)* or *sams-4(RNAi)* at 15°C. **(E)** Aggregation plots showing TSS enrichment in the H3K4me3 peaks identified in animals fed control RNAi or *sams-1(RNAi)* or *sams-4(RNAi)* at 15°C and Venn diagram comparing the overlap in the H3K4me3 peaks identified in animals fed control RNAi or *sams-1(RNAi)* or *sams-4(RNAi)* at 37°C. **(F)** Bubble chart showing enriched gene categories in differential peaks as determined by WormCat in animals fed control RNAi at 15°C only, 37°C only and common between 15°C and 37°C (**G**) or *sams-1(RNAi)* and *sams-4(RNAi)* at 37°C. Aggregation plots showing TSS enrichment in the *sams-1(RNAi)* and *sams-4(RNAi)* independent H3K4me3 peaks identified in animals fed control RNAi or *sams-1(RNAi)* or *sams-4(RNAi)* at **(H)** 15°C or **(I)** 37°C. Shaded areas in the Venn diagrams indicate the population of genes used for plotting the TSS enrichment plots. Aggregation plots showing TSS enrichment in the *sams-1(RNAi)* and *sams-4(RNAi)* dependent H3K4me3 peaks identified in animals fed control RNAi or *sams-1(RNAi)* or *sams-4(RNAi)* at **(J)** 15°C or **(K)** 37°C. Shaded areas in the Venn diagrams indicate the population of genes used for plotting the TSS enrichment plots.

Fig.3 Distinct gene expression and H3K4me3 patterns after heat shock in *sams-1* and *sams-4* RNAi animals

(A) Venn diagram showing overlap of genes upregulated by heat shock in control, *sams-1* or *sams-4* RNAi animals. *sams-1* data is from Ding, et al. 2018. **(B)** Bubble charts show broad category enrichment of up genes determined by Worm-Cat in control (RNAi) or *sams-1* or *sams-4* animals in genes changed (FDR<0.01) after heat shock. **(C)** Heat map for heat shock response genes up regulated following heat shock in animals fed control RNAi, *sams-1* or *sams-4(RNAi).* TSS plots showing aggregation of H3K4me3 in genes upregulated in control, *sams-1* or *sams-4* RNAi at **(D)** 15°C or **(E)** 37°C. TSS plots showing aggregation of H3K4me3 in all genes upregulated in control or *sams-1* dependent or *sams-4* RNAi dependent at **(F)** 15°C or **(G)** 37°C. Genome browser tracks for **(H)** *fbxa-59* and **(I)** *T27F6.8* to visualize changes in H3K4me3 enrichment in animals fed control, *sams-1* or *sams-4(RNAi)* at 15°C or 37°C.

Fig.4. *nhr* and lipid beta oxidation genes lose H3K4me3 after sams-1 RNAi but expression after heat shock

(A) Venn diagram showing overlap in down regulated genes in animals fed control, *sams-1* or *sams-4(RNAi)* at 37°C. **(B)** Bubble charts show broad category enrichment of metabolism genes determined by Worm-Cat in *sams-1* or *sams-4* animals in genes changed (FDR<0.01) after heat shock. **(C)** Bubble charts show broad category enrichment of transcription factor and metabolism genes determined by Worm-Cat in *sams-1* or *sams-4* animals in genes changed (FDR<0.01) after heat shock. Aggregation plots showing average enrichment of reads around the transcription start site (TSS) in

animals fed **(D)** control, **(E)** *sams-1* or **(F)** *sams-4(RNAi)* at 15°C or 37°C. Heat map for **(G)** nuclear hormone response genes and **(H)** lipid β-oxidation genes down regulated following heat shock in animals fed control RNAi, *sams-1* or *sams-4(RNAi)*. **(I)** Venn diagram showing the overlap between H3K4me3 peaks identified in animals fed control or *sams-1(RNAi)* at 15°C and down regulated genes identified in heat shocked animals fed *sams-1(RNAi*). (**J)** Genome browser tracks for *nhr-68* to visualize changes in H3K4me3 enrichment in animals fed control, *sams-1* or *sams-4(RNAi)* at 15°C or 37°C.

Supplemental data

Fig S1: Distinct patterns of gene expression after *sams-1 or sams-4* RNAi in basal conditions

(A) Absolute quantification of the SAM level in animals fed on control RNAi or sams-*4(RNAi).* The levels are expressed as mM/mg tissue. **(B)** Venn diagram showing the overlap in up regulated genes in animals fed *sams-1* or *sams-4(RNAi).* **(C)** Bubble charts show broad category enrichment of up regulated genes in animals fed *sams-1* or *sams-4(RNAi).* **(D)** Bubble charts show broad category enrichment of down regulated genes in animals fed *sams-1* or *sams-4(RNAi).* **(E)** Venn diagram showing the overlap in up regulated genes involved in lipid metabolism in animals fed *sams-1* or *sams-4(RNAi).* **(F)** Venn diagram showing the overlap in up regulated genes involved in pathogen stress response in animals fed *sams-1* or *sams-4(RNAi).* **(G)** Schematic for the heat stress assay. **(H)** Kaplan-Meier survival plots of animals fed *sams-4(RNAi)*.

Statistical significance is shown by Log-rank test. Assay was repeated thrice, and the graph represents the average of 3 biologically independent repeats.

Fig S2: H3K4me3 demethylases modulate SAM synthase phenotypes

(A) N2 or *sams-1(lof)* were grown on control RNAi or *set-2*(RNAi) and exposed to heat shock at adult stage. Survival was determined by plotting Kaplan-Meier survival plots. Statistical significance is shown by Log-rank test. Each assay was repeated thrice, and the graph represents the average of 3 biologically independent repeats. **(B)** Representative immunofluorescence images of intestinal nuclei stained with H3K4me3 specific antibody. Immunofluorescence staining was carried out to quantify the level of H3K4me3 in intestinal nuclei with and without heat shock in N2 or *sams-1(lof)* animals fed control RNAi or *set-2(RNAi)*. **(C),** Quantification of immunofluorescence imaging of intestinal nuclei stained with HK4me3 antibody after heat shock. Statistical significance was calculated using unpaired Student's t-test. ns= not significant, **** = $p<0.0001$, *** = $p<0.001$. Graph represents average of three biologically independent repeats per condition. **(D)** N2 or *sams-1(lof)* were grown on control RNAi or *set-16*(RNAi) and exposed to heat shock at adult stage. Survival was determined by plotting Kaplan-Meier survival plots. Statistical significance is shown by Log-rank test. Each assay was repeated thrice, and the graph represents the average of 3 biologically independent repeats. **(E)** Representative immunofluorescence images of intestinal nuclei stained with H3K4me3 specific antibody. Immunofluorescence staining was carried out to quantify the level of H3K4me3 in intestinal nuclei with and without heat shock in N2 or *sams-1(lof)* animals fed control RNAi or *set16(RNAi)*. **(F),** Quantification of

immunofluorescence imaging of intestinal nuclei stained with HK4me3 antibody after heat shock. Statistical significance was calculated using unpaired Student's t-test. ns= not significant, **** = p<0.0001, *** = p<0.001. Graph represents average of three biologically independent repeats per condition. **(G)** N2 or *sams-1(lof)* were grown on control RNAi or *rbr-2(RNAi)* or **(H)** *spr-5* and exposed to heat shock at adult stage. Survival was determined by plotting Kaplan-Meier survival plots. Statistical significance is shown by Log-rank test. Each assay was repeated thrice, and the graph represents the average of 3 biologically independent repeats. N2 or *sams-4(ok3315)* were grown on control RNAi, **(I)** *set-2*(RNAi) or **(J)** *set-16*(RNAi) and exposed to heat shock at adult stage. Survival was determined by plotting Kaplan-Meier survival plots. Statistical significance is shown by Log-rank test. Each assay was repeated thrice, and the graph represents the average of 3 biologically independent repeats

Fig S3. Distinct gene expression and H3K4me3 patterns after heat shock in *sams-1* and *sams-4* RNAi animals

Sunburst diagram showing the enriched gene categories in animals fed control RNAi at **(A)** 15°C or **(B)** 37°C. Sunburst diagram showing the overall enriched gene categories **(C)** and genes involved in metabolism **(D)** in animals fed *sams-1(RNAi)* at 37°C. Sunburst diagram showing the overall enriched gene categories **(E)** and genes involved in metabolism **(F)** in animals fed *sams-4(RNAi)* at 37°C. Aggregation plots showing average enrichment of reads around the transcription start site (TSS) for genes which are *sams-1* dependent only dependent on either *sams-1* or *sams-4* or *sams-4* dependent only at **(G)** 15°C or **(H)** 37°C.

Fig S4. Overlapping and distinct expression patterns of endogenously tagged *sams-1* and *sams-4*

(A) Representative immunofluorescence images of H3K4me3 staining in the germline in animals fed on control, *sams-1* or *sams-4(RNAi)*. **(B)** Venn diagrams showing the overlap in H3K4me3 peaks identified on ubiquitously expressed genes in control animals at 15°C or 37°C. **(C)** Venn diagrams showing the overlap in H3K4me3 peaks identified on germline specific genes in control animals at 15°C or 37°C. Aggregation plots showing average enrichment of reads around the transcription start site (TSS) of **(D)** ubiquitously or **(E)** germline specific or **(F)** intestine specific genes in animals fed control, *sams-1* or *sams-4(RNAi)* at 15°C.Aggregation plots showing average enrichment of reads around the transcription start site (TSS) of **(G)** ubiquitously or **(H)** germline specific or **(I)** intestine specific genes in animals fed control, *sams-1* or *sams-4(RNAi)* at 37°C. **(J)** Schematic showing the dynamic changes in the transcription and H3K4me3 landscape in low SAM animals following heat shock.

Table S1 (Microsoft Excel File) RNA seq for SAM synthase knockdown in basal conditions. Tabs A-C show *sams-3, sams-4, sams-5 (RNAi)* RNA seq data then **Tabs D-F** show WormCat gene enrichment. *sams-1* data is from Ding, et al. 2018. Enriched categories from WormCat. Red color denoted categories with a p value of less than 0.01 NS is not significant, NV is no value, RGS is regulated gene set.

Table S2 (Microsoft Excel File) Statistics for survival curves. Each tab contains data for replicate experiments (R1, R2, R3). Statistical information from GraphPad Prism is also included.

Table S3 (Microsoft Excel File). Tabs A-F: Cut and Tag peaks from Control, *sams-1* and *sams-4* RNAi animals at 15 and 37 degrees determined by HOMER. **Tabs G-I:** Enriched categories from WormCat. Color denoted categories with a p value of less than 0.01 NS is not significant, NV is no value, RGS is regulated gene set.

Table S4 (**Microsoft Excel File). Limited activation of heat shock response in *sams-4* RNAi animals.** Tabs show RNA seq from control (**A**), *sams-1* (**B**) *or sams-4* **(C**) animals subjected to heat shock that was used for comparison with C&T data. Differential genes were identified using Deseq2 in DolphinNext. Data for control and *sams-1* RNAi animals is from Ding, et al 2018. WormCat batch output of two-fold regulated genes for Categories 1, 2 and 3 are in tabs E-G). Highlighting denotes genes with significantly p values. NS is not significant, NV is no value, RGS is regulated gene set.

References

Alvares, S.M., Mayberry, G.A., Joyner, E.Y., Lakowski, B., and Ahmed, S. (2014). H3K4 demethylase activities repress proliferative and postmitotic aging. Aging Cell *13*, 245 253.

Annibal, A., Tharyan, R.G., Schonewolff, M.F., Tam, H., Latza, C., Auler, M.M.K., Grönke, S., Partridge, L., and Antebi, A. (2021). Regulation of the one carbon folate cycle as a shared metabolic signature of longevity. Nat Commun *12*, 3486.

Arda, H.E., Taubert, S., MacNeil, L.T., Conine, C.C., Tsuda, B., Gilst, M.V., Sequerra, R., Doucette-Stamm, L., Yamamoto, K.R., and Walhout, A.J.M. (2010). Functional modularity of nuclear hormone receptors in a *Caenorhabditis elegans* metabolic gene regulatory network. Mol Syst Biol *6*, 367.

Bannister, A.J., and Kouzarides, T. (2011). Regulation of chromatin by histone modifications. Cell Res *21*, 381–395.

Bulcha, J.T., Giese, G.E., Ali, Md.Z., Lee, Y.-U., Walker, M.D., Holdorf, A.D., Yilmaz, L.S., Brewster, R.C., and Walhout, A.J.M. (2019). A Persistence Detector for Metabolic Network Rewiring in an Animal. Cell Reports *26*, 460-468.e4.

Cheng, C., and Kurdistani, S.K. (2022). Chromatin as a metabolic organelle: Integrating the cellular flow of carbon with gene expression. Mol Cell *82*, 8–9.

Dai, Z., Mentch, S.J., Gao, X., Nichenametla, S.N., and Locasale, J.W. (2018). Methionine metabolism influences genomic architecture and gene expression through H3K4me3 peak width. Nat Commun *9*, 1955.

Das, S., Min, S., and Prahlad, V. (2021). Gene bookmarking by the heat shock transcription factor programs the insulin-like signaling pathway. Mol Cell *81*, 4843-4860.e8.

Ding, W., Smulan, L.J., Hou, N.S., Taubert, S., Watts, J.L., and Walker, A.K. (2015). s-Adenosylmethionine Levels Govern Innate Immunity through Distinct Methylation-Dependent Pathways. Cell Metab *22*, 633 645.

Ding, W., Higgins, D.P., Yadav, D.K., Godbole, A.A., Pukkila-Worley, R., and Walker, A.K. (2018). Stress-responsive and metabolic gene regulation are altered in low S-adenosylmethionine. Plos Genet *14*, e1007812.

Ducker, G.S., and Rabinowitz, J.D. (2016). One-Carbon Metabolism in Health and Disease. Cell Metab *25*.

Eissenberg, J.C., and Shilatifard, A. (2010). Histone H3 lysine 4 (H3K4) methylation in development and differentiation. Dev Biol *339*, 240 249.

Gao, X., Sanderson, S.M., Dai, Z., Reid, M.A., Cooper, D.E., Lu, M., Richie, J.P., Ciccarella, A., Calcagnotto, A., Mikhael, P.G., et al. (2019). Dietary methionine links nutrition and metabolism to the efficacy of cancer therapies. Nature *572*, 397–401.

Greco, C.M., Cervantes, M., Fustin, J.-M., Ito, K., Ceglia, N., Samad, M., Shi, J., Koronowski, K.B., Forne, I., Ranjit, S., et al. (2020). S-adenosyl-l-homocysteine hydrolase links methionine metabolism to the circadian clock and chromatin remodeling. Sci Adv *6*, eabc5629.

Greer, E.L., Maures, T.J., Hauswirth, A.G., Green, E.M., Leeman, D.S., Maro, G.S., Han, S., Banko, M.R., Gozani, O., and Brunet, A. (2010). Members of the H3K4 trimethylation complex regulate lifespan in a germline-dependent manner in *C. elegans*. Nature *466*, 383 387.

Han, S., and Brunet, A. (2012). Histone methylation makes its mark on longevity. Trends Cell Biol *22*, 42–49.

Han, S., Schroeder, E.A., Silva-García, C.G., Hebestreit, K., Mair, W.B., and Brunet, A. (2017). Mono-unsaturated fatty acids link H3K4me3 modifiers to *C. elegans* lifespan. Nature *544*, 185 190.

Hansen, M.H.A.L.D.A.K.C. (2005). New Genes tied to Endocrine, Metabolic and Dietary Regulation of Lifespan from a *Caenorhabditis elegans* RNAi Screen. Cell *1*, 119 128.

Harris, T.W., Arnaboldi, V., Cain, S., Chan, J., Chen, W.J., Cho, J., Davis, P., Gao, S., Grove, C.A., Kishore, R., et al. (2019). WormBase: a modern Model Organism Information Resource. Nucleic Acids Res *48*, D762–D767.

Heinz, S., Benner, C., Spann, N., Bertolino, E., Lin, Y.C., Laslo, P., Cheng, J.X., Murre, C., Singh, H., and Glass, C.K. (2010). Simple Combinations of Lineage-Determining Transcription Factors Prime cis-Regulatory Elements Required for Macrophage and B Cell Identities. Mol Cell *38*, 576–589.

Hödl, M., and Basler, K. (2012). Transcription in the Absence of Histone H3.2 and H3K4 Methylation. Curr Biol *22*, 2253 2257.

Hoffert, K.M., Higginbotham, K.S.P., Gibson, J.T., Oehrle, S., and Strome, E.D. (2019). Mutations in the S-adenosylmethionine Synthetase Genes, SAM1 and SAM2, Differentially Impact Genome Stability in *Saccharomyces cerevisiae*. Genetics *213*, genetics.302435.2019.

Holdorf, A.D., Higgins, D.P., Hart, A.C., Boag, P.R., Pazour, G.J., Walhout, A.J.M., and Walker, A.K. (2019). WormCat: An Online Tool for Annotation and Visualization of *Caenorhabditis elegans* Genome-Scale Data. Genetics genetics.302919.2019.

Hsieh, W.-C., Sutter, B.M., Ruess, H., Barnes, S.D., Malladi, V.S., and Tu, B.P. (2022). Glucose starvation induces a switch in the histone acetylome for activation of gluconeogenic and fat metabolism genes. Mol Cell *82*, 60-74.e5.

Hulsen, T., Vlieg, J. de, and Alkema, W. (2008). BioVenn – a web application for the comparison and visualization of biological lists using area-proportional Venn diagrams. Bmc Genomics *9*, 488.

Kaletsky, R., Yao, V., Williams, A., Runnels, A.M., Tadych, A., Zhou, S., Troyanskaya, O.G., and Murphy, C.T. (2018). Transcriptome analysis of adult *Caenorhabditis elegans* cells reveals tissue-specific gene and isoform expression. Plos Genet *14*, e1007559.

Kaya-Okur, H.S., Wu, S.J., Codomo, C.A., Pledger, E.S., Bryson, T.D., Henikoff, J.G., Ahmad, K., and Henikoff, S. (2019a). CUT&Tag for efficient epigenomic profiling of small samples and single cells. Nat Commun *10*, 1930.

Kraus, D., Yang, Q., Kong, D., Banks, A.S., Zhang, L., Rodgers, J.T., Pirinen, E., Pulinilkunnil, T.C., Gong, F., Wang, Y., et al. (2014). Nicotinamide N-methyltransferase knockdown protects against diet-induced obesity. Nature *508*, 258 262.

Kucukural, A., Yukselen, O., Ozata, D.M., Moore, M.J., and Garber, M. (2019). DEBrowser: interactive differential expression analysis and visualization tool for count data. Bmc Genomics *20*, 6.

Langmead, B., Trapnell, C., Pop, M., and Salzberg, S.L. (2009). Ultrafast and memory-efficient alignment of short DNA sequences to the human genome. Genome Biol *10*, R25–R25.

Li, T., and Kelly, W.G. (2011). A role for Set1/MLL-related components in epigenetic regulation of the Caenorhabditis elegans germ line. Plos Genet *7*, e1001349.

Li, S., Swanson, S.K., Gogol, M., Florens, L., Washburn, M.P., Workman, J.L., and Suganuma, T. (2015). Serine and SAM Responsive Complex SESAME Regulates Histone Modification Crosstalk by Sensing Cellular Metabolism. Mol Cell *60*, 408 421.

Liu, M., and Pile, L.A. (2017). The Transcriptional Corepressor SIN3 Directly Regulates Genes Involved in Methionine Catabolism and Affects Histone Methylation, Linking Epigenetics and Metabolism*. J Biol Chem *292*, 1970–1976.

Lu, S.C., Alvarez, L., Huang, Z.-Z., Chen, L., An, W., Corrales, F.J., Avila, M.A., Kanel, G., and Mato, J.M. (2001). Methionine adenosyltransferase 1A knockout mice are

predisposed to liver injury and exhibit increased expression of genes involved in proliferation. Proc National Acad Sci *98*, 5560–5565.

Lussi, Y.C., Mariani, L., Friis, C., Peltonen, J., Myers, T.R., Krag, C., Wong, G., and Salcini, A.E. (2016). Impaired removal of H3K4 methylation affects cell fate determination and gene transcription. Development *143*, 3751 3762.

Mahat, D.B., Salamanca, H.H., Duarte, F.M., Danko, C.G., and Lis, J.T. (2016). Mammalian Heat Shock Response and Mechanisms Underlying Its Genome-wide Transcriptional Regulation. Mol Cell *62*, 63 78.

Maldonado, L.Y., Arsene, D., Mato, J.M., and Lu, S.C. (2018). Methionine adenosyltransferases in cancers: Mechanisms of dysregulation and implications for therapy. Exp Biol Med *243*, 107–117.

Mato, J.M., Corrales, F.J., Lu, S.C., and Avila, M.A. (2002). S-Adenosylmethionine: a control switch that regulates liver function. FASEB Journal *16*, 15 26.

Mato, J.M., Martínez-Chantar, M.L., and Lu, S.C. (2008). Methionine Metabolism and Liver Disease. Annu Rev Nutr *28*, 273 293.

McGhee, J. (2007). The *C. elegans* intestine. Wormbook 1–36.

Mentch, S.J., and Locasale, J.W. (2016). One-carbon metabolism and epigenetics: understanding the specificity. Ann Ny Acad Sci *1363*, 91 98.

Mentch, S.J., Mehrmohamadi, M., Huang, L., Liu, X., Gupta, D., Mattocks, D., Gómez Padilla, P., Ables, G., Bamman, M.M., Thalacker-Mercer, A.E., et al. (2015). Histone Methylation Dynamics and Gene Regulation Occur through the Sensing of One-Carbon Metabolism. Cell Metab *22*.

Morimoto, R.I. (2006). Stress, Aging, and Neurodegenerative Disease. New Engl J Medicine *355*, 2254–2255.

Murray, B., Barbier-Torres, L., Fan, W., Mato, J.M., and Lu, S.C. (2019). Methionine adenosyltransferases in liver cancer. World J Gastroentero *25*, 4300–4319.

Nadal, E. de, Ammerer, G., and Posas, F. (2011). Controlling gene expression in response to stress. Nat Rev Genet *12*, 833–845.

Parkhitko, A.A., Jouandin, P., Mohr, S.E., and Perrimon, N. (2019). Methionine metabolism and methyltransferases in the regulation of aging and lifespan extension across species. Aging Cell *18*, e13034.

Serizay, J., Dong, Y., Janes, J., Chesney, M., Cerrato, C., and Ahringer, J. (2020). Distinctive regulatory architectures of germline-active and somatic genes in *C. elegans*. Genome Res gr.265934.120.

Shilatifard, A. (2012). The COMPASS family of histone H3K4 methylases: mechanisms of regulation in development and disease pathogenesis. Annu Rev Biochem *81*, 65 95.

Shyh-Chang, N., Locasale, J.W., Lyssiotis, C.A., Zheng, Y., Teo, R.Y., Ratanasirintrawoot, S., Zhang, J., Onder, T., Unternaehrer, J.J., Zhu, H., et al. (2013). Influence of Threonine Metabolism on *S*-Adenosylmethionine and Histone Methylation. Science *339*, 222 226.

Sullivan, M.R., Darnell, A.M., Reilly, M.F., Kunchok, T., Joesch-Cohen, L., Rosenberg, D., Ali, A., Rees, M.G., Roth, J.A., Lewis, C.A., et al. (2021). Methionine synthase is essential for cancer cell proliferation in physiological folate environments. Nat Metabolism *3*, 1500–1511.

Sun, Y., and Locasale, J.W. (2021). Rethinking the bioavailability and cellular transport properties of S-adenosylmethionine. Cell Stress *6*, 1–5.

Tang, S., Fang, Y., Huang, G., Xu, X., Padilla-Banks, E., Fan, W., Xu, Q., Sanderson, S.M., Foley, J.F., Dowdy, S., et al. (2017). Methionine metabolism is essential for SIRT1-regulated mouse embryonic stem cell maintenance and embryonic development. Embo J *36*, 3175–3193.

Towbin, B.D., González-Aguilera, C., Sack, R., Gaidatzis, D., Kalck, V., Meister, P., Askjaer, P., and Gasser, S.M. (2012). Step-wise methylation of histone H3K9 positions heterochromatin at the nuclear periphery. Cell *150*, 934 947.

Walker, A.K., Jacobs, R.L., Watts, J.L., Rottiers, V., Jiang, K., Finnegan, D.M., Shioda, T., Hansen, M., Yang, F., Niebergall, L.J., et al. (2011). A Conserved SREBP-1/Phosphatidylcholine Feedback Circuit Regulates Lipogenesis in Metazoans. Cell *147*, 840 852.

Walsh, C.T., Tu, B.P., and Tang, Y. (2017). Eight Kinetically Stable but Thermodynamically Activated Molecules that Power Cell Metabolism. Chem Rev *118*, acs.chemrev.7b00510.

Weiner, A., Chen, H.V., Liu, C.L., Rahat, A., Klien, A., Soares, L., Gudipati, M., Pfeffner, J., Regev, A., Buratowski, S., et al. (2012). Systematic dissection of roles for chromatin regulators in a yeast stress response. Plos Biol *10*, e1001369.

Wellen, K.E., Hatzivassiliou, G., Sachdeva, U.M., Bui, T.V., Cross, J.R., and Thompson, C.B. (2009). ATP-Citrate Lyase Links Cellular Metabolism to Histone Acetylation. Science *324*, 1076 1080.

Wenzel, D., Palladino, F., and Jedrusik-Bode, M. (2011). Epigenetics in *C. elegans*: facts and challenges. Genesis *49*, 647 661.

Xiao, Y., Bedet, C., Robert, V.J.P., Simonet, T., Dunkelbarger, S., Rakotomalala, C., Soete, G., Korswagen, H.C., Strome, S., and Palladino, F. (2011). *Caenorhabditis elegans* chromatin-associated proteins SET-2 and ASH-2 are differentially required for histone H3 Lys 4 methylation in embryos and adult germ cells. Proc National Acad Sci *108*, 8305 8310.

Ye, C., and Tu, B.P. (2018). Sink into the Epigenome: Histones as Repositories That Influence Cellular Metabolism. Trends Endocrinol Metabolism *29*, 626 637.

Yukselen, O., Turkyilmaz, O., Ozturk, A.R., Garber, M., and Kucukural, A. (2020). DolphinNext: a distributed data processing platform for high throughput genomics. Bmc Genomics *21*, 310.

Zhu, L.J., Gazin, C., Lawson, N.D., Pagès, H., Lin, S.M., Lapointe, D.S., and Green, M.R. (2010). ChIPpeakAnno: a Bioconductor package to annotate ChIP-seq and ChIP-chip data. Bmc Bioinformatics *11*, 237–237.

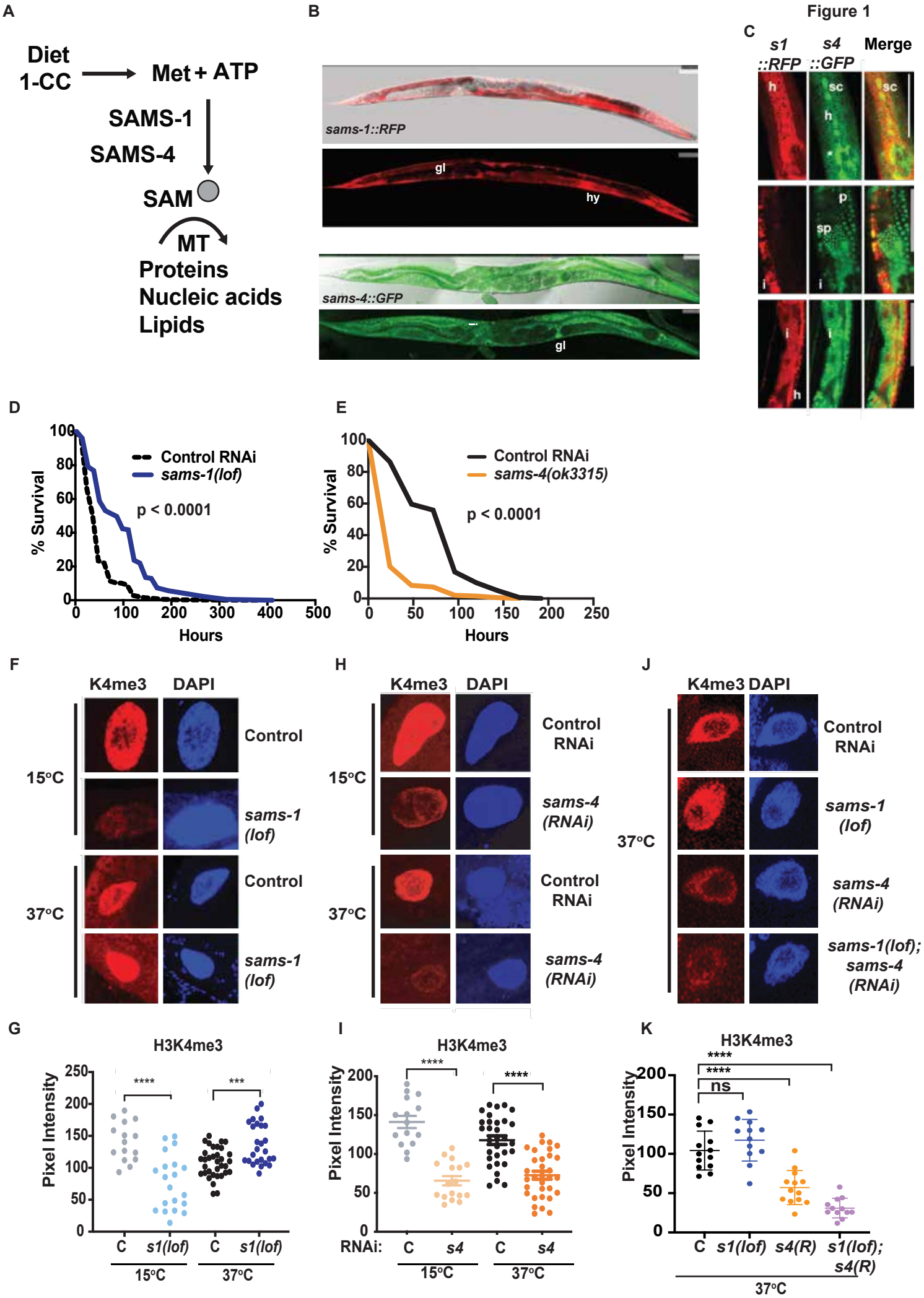
A
Diet
1-CC
Met + ATP
SAMS-1
SAMS-4
SAM
MT
Proteins
Nucleic acids
Lipids
B
sams-1::RFP
gl
hy
sams-4::GFP
gl
C
s1 ::RFP
s4 ::GFP
Merge
h
sc
h
sc
p
sp
i
i
i
i
h
D
% Survival
Hours
Control RNAi
sams-1(lof)
p < 0.0001
E
% Survival
Hours
Control RNAi
sams-4(ok3315)
p < 0.0001
F
K4me3
DAPI
15°C
37°C
Control
sams-1 (lof)
Control
sams-1 (lof)
H
K4me3
DAPI
15°C
37°C
Control RNAi
sams-4 (RNAi)
Control RNAi
sams-4 (RNAi)
J
K4me3
DAPI
37°C
Control RNAi
sams-1 (lof)
sams-4 (RNAi)
sams-1(lof); sams-4 (RNAi)
G
H3K4me3
Pixel Intensity
****
***
C
s1(lof)
C
s1(lof)
15°C
37°C
I
H3K4me3
Pixel Intensity
****
****
RNAi:
C
s4
C
s4
15°C
37°C
K
H3K4me3
Pixel Intensity
****
****
ns
C
s1(lof)
s4(R)
s1(lof); s4(R)
37°C

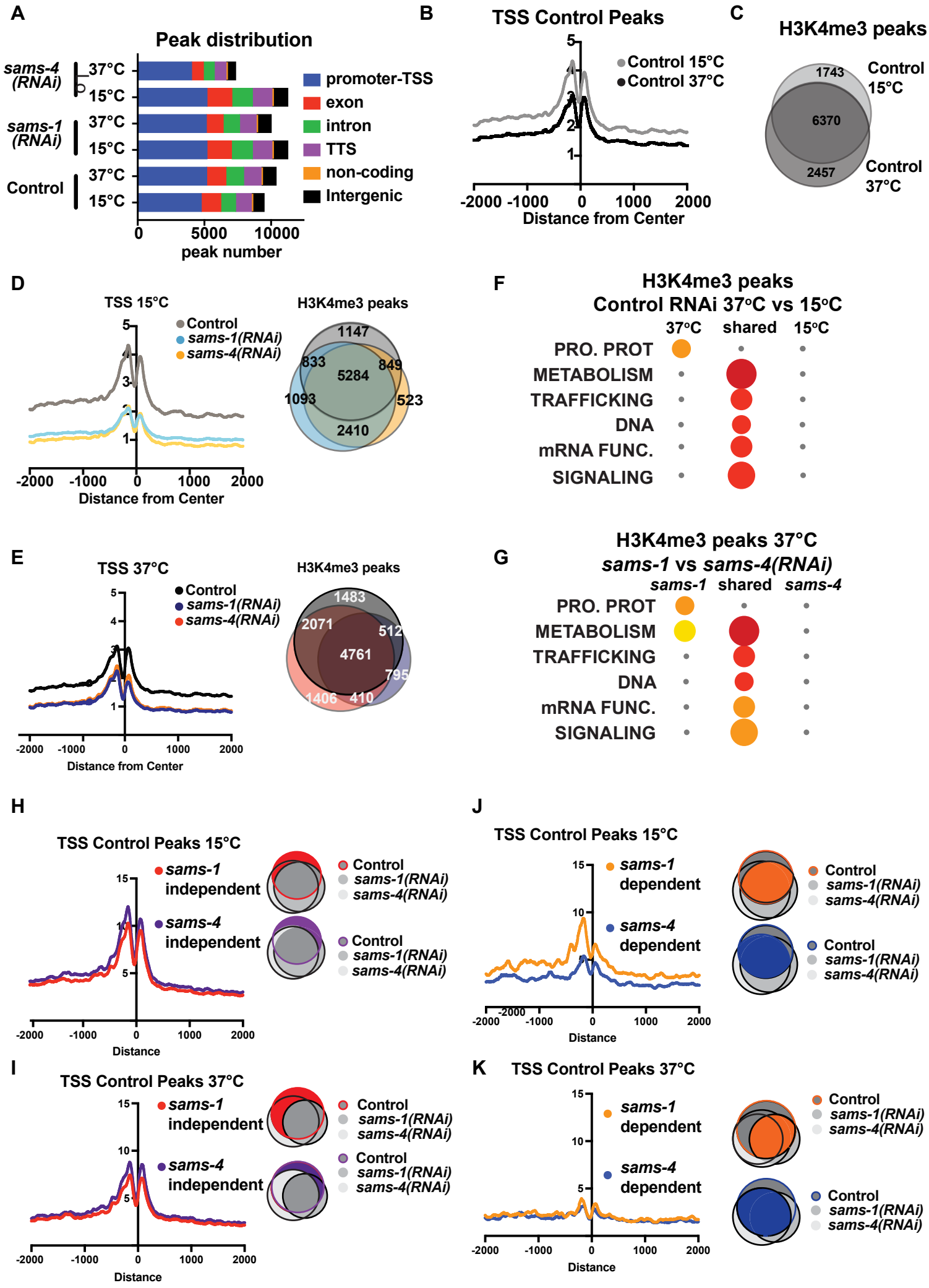
A
Peak distribution
sams-4 (RNAi)
37°C
15°C
sams-1 (RNAi)
37°C
15°C
Control
37°C
15°C
promoter-TSS
exon
intron
TTS
non-coding
Intergenic
0
5000
10000
peak number
B
TSS Control Peaks
Control 15°C
Control 37°C
-2000 -1000 0 1000 2000
Distance from Center
C
H3K4me3 peaks
1743
6370
2457
Control 15°C
Control 37°C
D
TSS 15°C
Control
sams-1(RNAi)
sams-4(RNAi)
-2000 -1000 0 1000 2000
Distance from Center
H3K4me3 peaks
1147
833
849
5284
1093
523
2410
E
TSS 37°C
Control
sams-1(RNAi)
sams-4(RNAi)
-2000 -1000 0 1000 2000
Distance from Center
H3K4me3 peaks
1483
2071
512
4761
795
1406
410
F
H3K4me3 peaks
Control RNAi 37°C vs 15°C
37°C
shared
15°C
PRO. PROT
METABOLISM
TRAFFICKING
DNA
mRNA FUNC.
SIGNALING
G
H3K4me3 peaks 37°C
sams-1 vs sams-4(RNAi)
sams-1
shared
sams-4
PRO. PROT
METABOLISM
TRAFFICKING
DNA
mRNA FUNC.
SIGNALING
H
TSS Control Peaks 15°C
sams-1 independent
sams-4 independent
Control
sams-1(RNAi)
sams-4(RNAi)
-2000 -1000 0 1000 2000
Distance
I
TSS Control Peaks 37°C
sams-1 independent
sams-4 independent
Control
sams-1(RNAi)
sams-4(RNAi)
-2000 -1000 0 1000 2000
Distance
J
TSS Control Peaks 15°C
sams-1 dependent
sams-4 dependent
Control
sams-1(RNAi)
sams-4(RNAi)
-2000 -1000 0 1000 2000
Distance
K
TSS Control Peaks 37°C
sams-1 dependent
sams-4 dependent
Control
sams-1(RNAi)
sams-4(RNAi)
-2000 -1000 0 1000 2000
Distance

Godbole et al
Figure 3

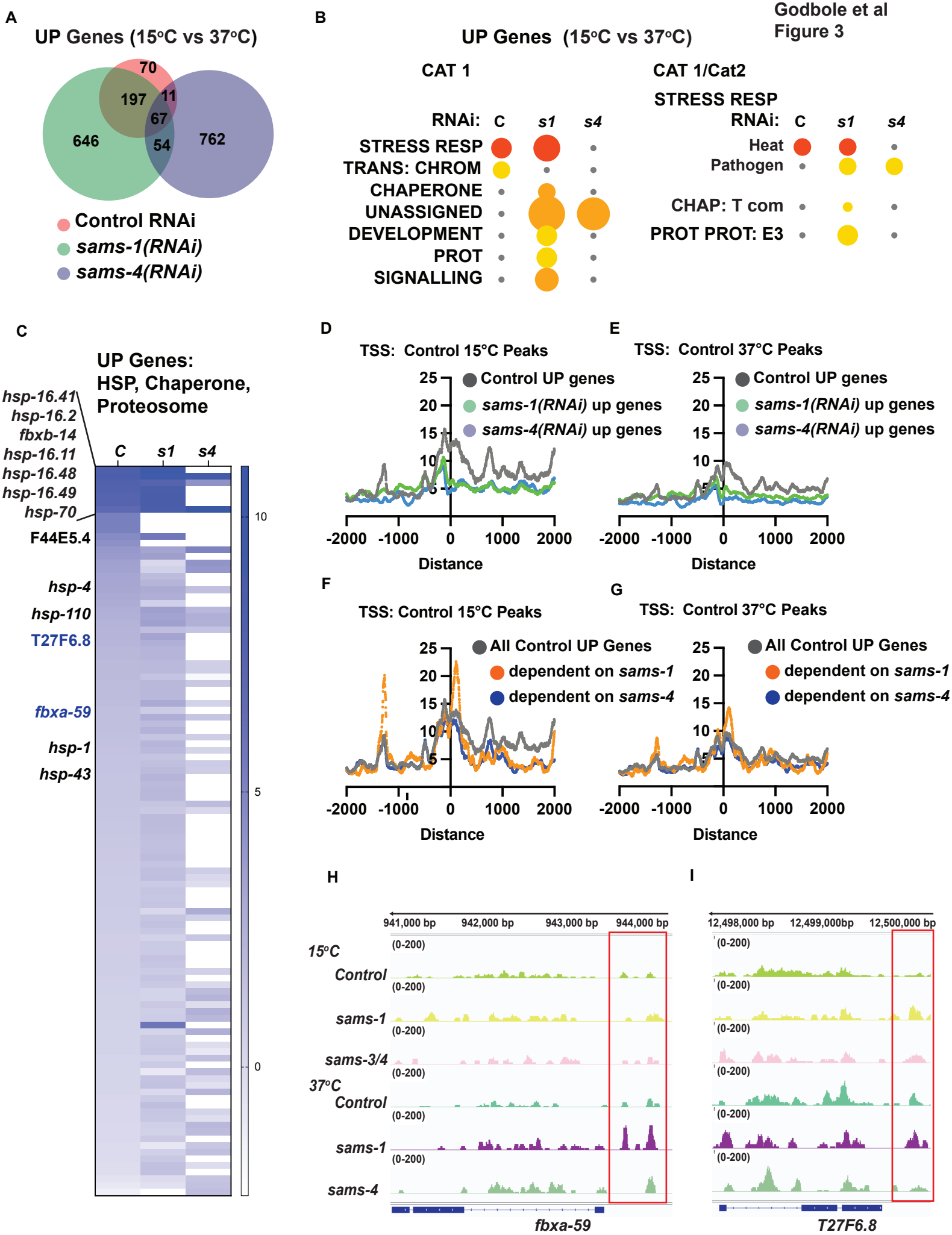
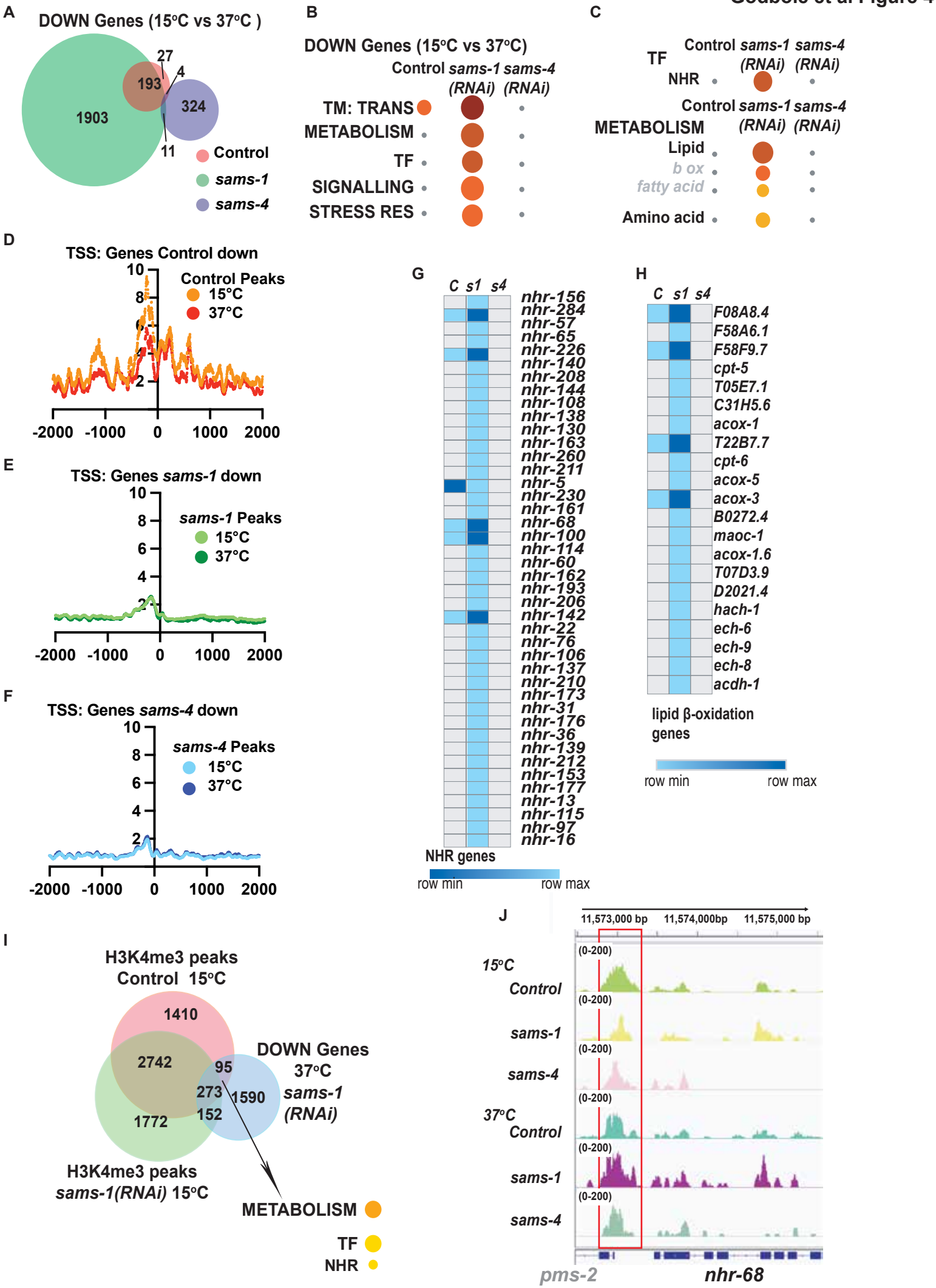
Godbole et al Figure 4